# Mac S-Design

MAKE YOUR SLOPE SAFER

## Scientific Manual

Version 1.0 – July 2021

MACCAFERRI

Engineering a Better Solution

# Table of Contents

# 1 Introduction

Officine Maccaferri has been active in the prevention of Hydrogeological Disasters since the late 19th century. It is a multinational company with more than 3000 employees, numerous production sites around the world and presence in more than 100 countries. It has developed various systems for the mitigation of Natural Hazards, based on its long and worldwide expertise.

The use of steel meshes on slopes to mitigate the risk of surficial failures has been a company practice since the middle of the 20th century, with both pinned and drapery solutions. The design and understanding of such solutions has been a company asset since the beginning, and the constant development of knowledge has been key part of the history of the company.

In recent years, with the help of the development of sound geotechnical numerical codes, it has become possible to investigate the interaction between the soil slope and the stabilising mesh. Furthermore, the understanding of the mechanical behaviour of the mesh derived from standard tests has helped to identify the key parameters needed to properly model the mesh.

For professionals the commonly available software use Limit Equilibrium Models, where the protection mesh is supposed to behave like a ‘wall’, i.e. a rigid structure able to develop the required resisting force and to transfer moment, independently of the deformation field involved. On the contrary, real-world experience and practice showed that a mesh can withstand huge deformations and that the stabilizing force it provides is highly dependent on the soil-mesh interaction and on the displacement field.

To keep both the approach and software as simple as possible and to avoid the need of advanced numerical software, a “hybrid” method has been chosen, by combining classical Limit Equilibrium Methods (to run the stability analyses) with an innovative displacement-controlled approach (to evaluate the stabilizing force provided by the mesh).

It is finally important to underline how this software is not conceived as a general stability analysis tool (i.e. it does not investigate all the possible failure surfaces in the slope, looking for the critical one); for a given depth of an unstable layer, its surficial stability is studied, with and without a pinned drapery system. The global stability analysis for the soil slope under investigation must be addressed with a tool specifically designed for this aim, such as MacStars W 4.0. Once the deep-seated global stability is addressed, then Mac S-Design is used to design the appropriate mesh system to overcome surficial instability.

# 2 Design approach

The design of stabilizing structures for potentially unstable slopes is a complex multiscale problem, since it involves the *local scale* of the representative elementary volume of soil (REV), the *macro scale* of the structure and the *mega scale* of the entire slope, as it is schematically shown in Figure 1 with reference to the case of piles stabilizing the slope. Usual numerical codes are often based on finite element or finite difference schemes. Although they are very efficient from a numerical point of view and they include advanced constitutive relationships for soils and rocks, they cannot tackle such a large variety of spatial scales. They often require large computational effort and advanced numerical and modelling skills from the user. They cannot be considered as rapid and simple design tools, especially in the preliminary dimensioning phase of the intervention (when a large number of parametrical analyses is usually required), or for small projects, where the time and the resources are generally very limited.

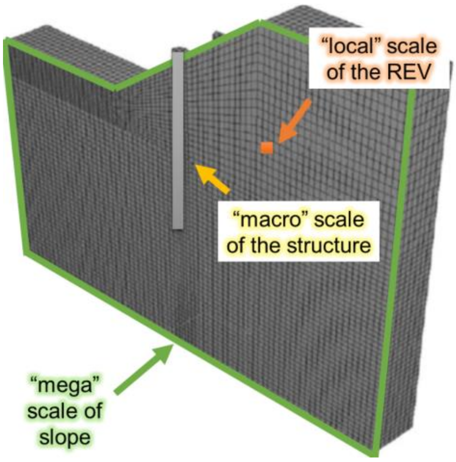


*Figure 1. Multiscale problem.*

In the following paragraphs, an alternative design procedure based on a sub-structuring approach is adopted with specific reference to passive anchored wire meshes for potentially unstable surficial layers of granular materials. The behaviour of each component of the system (i.e. the individual failure mechanisms of the slope, the stabilizing system, the local soil-mesh interaction, etc.) is studied separately by adopting specific constitutive relationships; the global behaviour at the mega scale is then obtained once equilibrium and compatibility is achieved across all the components.

## 2.1 Assumptions

With reference to the simplified sketch for the reinforcement of the unstable surficial layer of a soil slope shown in Figure 2a, the sub-structuring approach allows engineers to study the stability of the surficial soil mass separately from other structural components. This soil mass is subject to the self-weight $W$, the shear force $T$ mobilized along its failure surface and the stabilizing contact pressure $q$ arising between the mesh and the slope profile (Figure 2b). In general, no initial pre-stressing action is imposed to the anchors (passive intervention systems are only considered here as it is not possible to apply a pre-stress or active pressure to a slope using any flexible mesh system), and the contact pressure $q$ is uniquely mobilized upon the activation of a local normal displacement $U_N$ of the soil. As a consequence, a relationship $q = q(U_N)$ is introduced. From a structural point of view, the anchored wire mesh is then subjected to a displacement-controlled loading process, governed by the normal component $U_N$ of the underlying soil displacement profile (Figure 2c and d). In the following, for the sake of simplicity, the axial deformability of the anchors will be disregarded with respect to soil and mesh deformability, and the mesh anchoring points will then be considered as fixed.

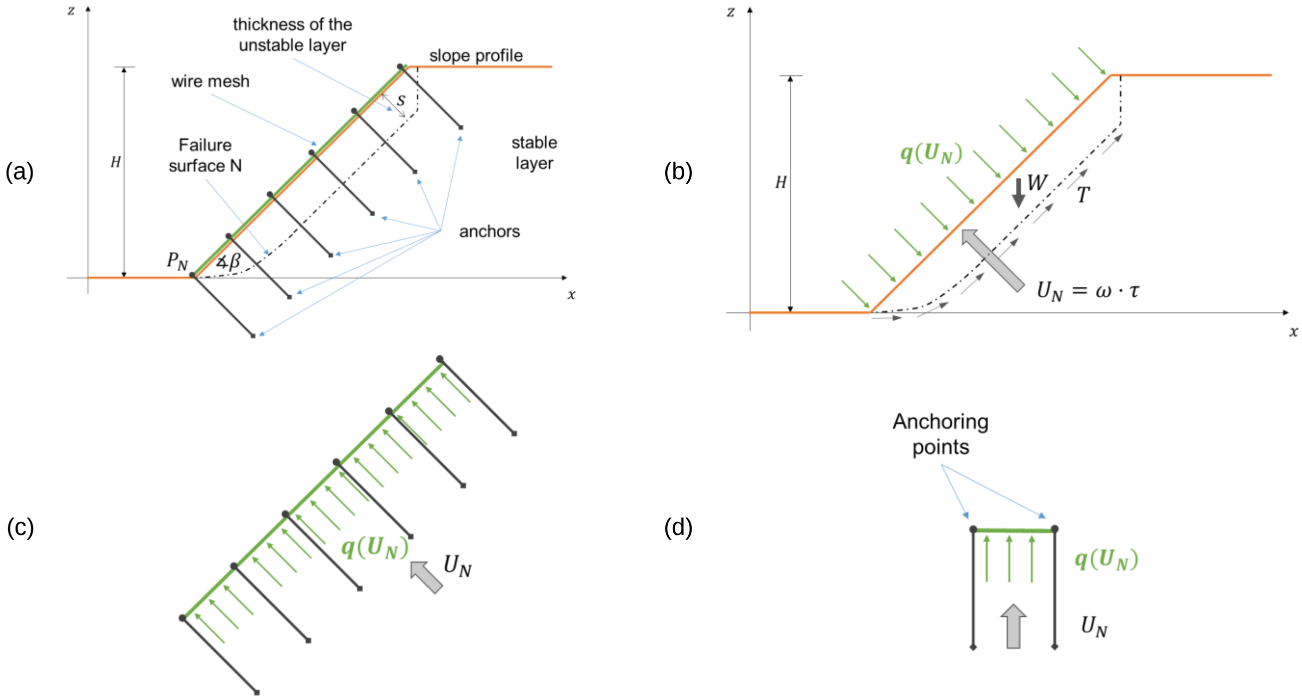


*Figure 2. (a) sketch an unstable slope reinforced with a passive anchored wire mesh; (b) stability analyses of the soil mass; (c) distributed contact pressure at the soil-mesh interface; (d) study of a single span of the mesh.*

A key role in the innovative Mac S-Design method is represented by the explicit definition of the relationship $q = q(U_N)$, named hereafter as “characteristic curve” of the system. The fundamental importance of the characteristic curve (whose derivation will be described in the following chapters) is that it represents a “generalized” constitutive law for each span of the mesh and for the underlying soil (i.e. at the “macro” scale of the structure), reproducing the behaviour of this system from its in-use condition until its failure. This characteristic curve, as in all soil-structure interaction problems, strictly depends on both the deformability and the strength of the soil and the wire mesh. Indeed, only an appropriate description of this interaction enables an accurate quantitative evaluation of the stabilizing action, and, thus, the definition of safe design solutions. This is particularly important when highly deformable structures are considered, as it is for all steel meshes supplied on rolls. In this case, in fact, the peak value of the characteristic curve, representing the maximum stabilizing pressure $q$ that can be supported by a span of the mesh, is also strictly dependent on the relative stiffness between the mesh and the soil deformability. As a consequence, the failure of the system is largely affected by the deformability values too. The usual design methods often adopted in practice are generally based on simplified Ultimate Limit State approaches and they disregard the soil/mesh relative stiffness. This may then result in a largely inaccurate and potentially unsafe analysis.

Finally, as briefly recalled in the following paragraphs, the advantage of introducing a characteristic curve is also to allow a consistent assessment of the performance of the stabilizing system, by relating the desired safety level for the unstable surficial soil layer to the corresponding in-use condition of the mesh.

## 2.2 Limit Equilibrium Methods and Hybrid Methods

Standard Limit Equilibrium Methods (LEM) usually study the stability of a soil mass along a failure surface $F$ by adopting the following equation:

$$E_k^F = \frac{R_k^F}{F_S} + A_{k,lim}^F. \tag{1a}$$

expressing the equilibrium among the driving action ($E$, generally given by the weight of the unstable soil mass), the mobilized soil strength ($R$) and the limit value of the stabilizing action ($A$) provided by the stabilizing intervention. In equation (1a), all the three terms are computed with reference to a specific failure mechanism (superscript index $F$) and by adopting the characteristic values of the mechanical parameters (subscript index $k$) and a safety factor $F_S$ is also introduced as a soil strength reduction factor. Alternatively, the same equation could also be written with reference to the design values of the cited quantities, once partial safety factors are introduced depending on the adopted design standards. The following inequality is hence written:

$$E_d^F < R_d^F + A_{d,lim}^F. \tag{1b}$$

In both cases, the contribution of the stabilizing structure is only considered at its limit condition, coinciding with the peak value (in case of 'brittle' systems) or with the ultimate asymptotic value (for ductile systems), without explicitly modelling the soil-mesh interaction. No direct relationship can be then argued between the safety level of the slope, the working condition of the mesh and the soil displacement.

On the contrary, starting from the sub-structuring approach schematically outlined in the previous paragraph, an innovative analysis method based on a "hybrid" approach will be adopted (see e.g. Galli et al., 2017, for a detailed description of such multilevel design approaches, with particular reference to slope stabilizing piles). The key concept is that the equilibrium of the soil mass is still analysed by means of usual LEM, but the stabilizing action provided by the passive structural intervention is expressed as a function of the relative soil-structure displacement. In other words, Hybrid Methods combine an Ultimate Limit State approach (ULS) with respect to soil strength to analyse the stability of the slope, with a Serviceability Limit State approach (SLS) with respect to the soil-structure interaction. This approach is consistent with the idea of dealing with *prevention interventions*, i.e. to design structures aimed at preventing the triggering of a failure mechanism in the slope, but allowing small pre-failure soil displacements, sufficient to activate the soil-mesh interaction.

From a computational point of view, it should be noted that, as it is usually done in common LEM, the equilibrium of the potential unstable soil mass will be studied with reference to a small-displacement scheme, i.e. by neglecting slope movements and writing the global equilibrium equations for the soil mass with respect to its initial undeformed state. On the contrary, the local soil-mesh interaction giving rise to the $q = q(U_N)$ curve, will be necessarily studied by adopting a large-displacement scheme, in order to correctly capture the membrane behaviour of the mesh, as will be discussed in §4.

The formal governing equation can then be simply written in the general form as follows:

$$E_k^F = \frac{R_k^F}{F_S} + A_k^F(\boldsymbol{U}), \tag{2}$$

extending the validity of equation (1a) to hybrid methods, through the definition of a "characteristic" function of the system $A = A(\boldsymbol{U})$, expressing the development of the global stabilizing action $A$ (in this case, the integral of the mobilized contact pressures $q$ between the slope profile and the mesh) with the displacement field $\boldsymbol{U}$ of the slope. As already pointed out, the key concepts derived from the introduction of such a characteristic function are that:

(a) the influence of the soil-mesh relative stiffness on the stabilizing force (affecting also its peak strength value) can be explicitly captured,

(b) the safety level of the surficial soil layer of the slope in the presence of the stabilizing system becomes a function of the soil displacement pattern, and

(c) the working condition of the mesh for the desired safety level of the unstable surficial layer can be explicitly evaluated.

Equation (2), conceptually introduces a relationship between the safety level (generally expressed as $F_S$) and the soil displacement field (Figure 3). Starting from the initial pre-intervention value of the safety factor $F_{S0}$, the designer can explicitly relate the chosen design value $F_{Sd}$ of the safety factor to the corresponding soil displacement amplitude, and to the working condition of the mesh. As an example, two cases of (i) a ductile and (ii) a brittle system are sketched, showing the two corresponding estimations of soil displacement amplitudes $U_{d(i)}$ and $U_{d(ii)}$. In this perspective, hybrid methods also represent an efficient methodology to rapidly compare alternative possible design solutions by adopting a consistent and safe performance-based criterion.

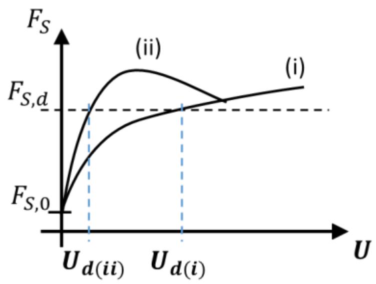


*Figure 3. Dependence of the slope safety factor $F_S$ on the soil displacement for (i) ductile and (ii) fragile stabilizing systems.*

Hybrid methods cannot however be used to foresee the long term behaviour of the system (e.g. the expected on-site displacement after the installation of the mesh), since they do not consider any time-evolution law of the system (equation (2) is in fact time interdependent). Furthermore, it shall be observed that, theoretically, a slide is triggered whenever $F_{S,0} < 1$, and the soil, as it is in all passive prevention systems, would continuously slide only until a new stable equilibrium condition is reached (i.e. $F_S = 1$). All the design conditions characterized by $F_{S,d} > 1$ cannot then ideally be reached in practice, and the displacement values $U_d$ computed by hybrid methods are therefore only meant as a measure of the performance of the system for a fixed safety level of the slope.

Finally, Hybrid Methods, as has already been briefly cited, are suitable for the design of ***prevention*** measures, conceptually referred to a pre-failure condition of the investigated instability (and in fact a proper safety factor with respect to its ultimate strength is introduced in the stability analyses). This is a fundamental difference with respect to ***protection*** measures, which are aimed at controlling the evolution of the phenomenon after the onset of a global failure mechanism. In this case, completely different computational tools would be required, based on large displacement approaches and capable of accounting relevant changes in the slope geometry (as it is, e.g., for debris flow protection interventions).

# 3 Slope analysis

With reference to the sub-structuring approach briefly outlined in §2.1, the main assumptions and the ideal geometry adopted for the stability analyses of the unstable surficial soil layer are discussed in the following paragraphs.

## 3.1 Main Assumptions

An illustration of the adopted ideal slope profile is presented in Figure 4. In particular, a slope of total height $H$, constituted by a homogeneous layer of granular material with uniform thickness $s$ and inclined of an angle $\beta$ along a stable deep layer, is considered. A water table at a uniform depth along the slope is present, and, depending on the mechanical properties of the unstable layer, tension cracks at the top of the slope may be considered.

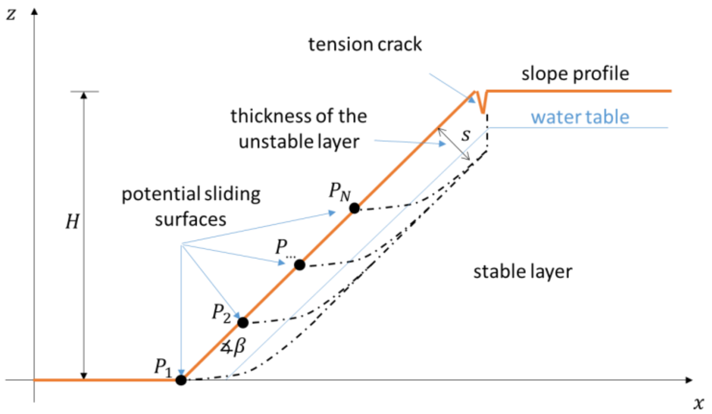


*Figure 4. Sketch of the considered slope profile.*

Only translational failure mechanisms of the unstable layer are considered, starting from the crest of the slope and extending until their emerging points $P$ along the slope. In general, $N$ failure surfaces (uniquely identified by points $P_i$ with $i = 1..N$) are defined. For the sake of completeness, two different approaches have been implemented, the first one (§3.2) is ideally more suited to steep slopes, whilst the second (§3.3) to more gentle slopes. Both approaches are simultaneously run in the analysis, and the solutions, consistent with usual LEM approaches, are derived by comparing all the considered failure mechanisms, and showing a suitable envelope of the results.

It is worth noting that both approaches are based on Limit Equilibrium assumptions, and that the difference between the two is limited to a different procedure for the evaluation of the toe stabilizing action provided to the unstable layer. Sections §3.2 and §3.3 respectively provide further details.

The governing parameters for the slope stability analysis are in general:

- Slope height ($H$)
- Slope inclination ($\beta$)
- Thickness of the unstable layer ($s$)
- Depth of the water table ($d_w$)

- Unit weight of the unstable layer, both below ($\gamma_{sat}$) and above the water table ($\gamma$)
- Friction angle ($\phi$)
- Cohesion ($c$)
- Tension crack ($z$)

The stabilizing effect provided by the anchors to the surficial unstable layer, modelled here as a simple additional resisting force parallel to the sliding plane, would actually require the definition of specific characteristic curves. In the following, however, for the sake of simplicity and owing to the minor contribution of this term to the overall stability of the slope, their effect is independently estimated by adopting a simplified analytical procedure, recently proposed by Di Laora et al. (2017) for slope stabilizing piles and based on an ULS approach. The contribution of nails to the global stability of the whole slope is then not considered through this approach.

In the considered method, the total resisting force provided by each single anchor to a transverse soil displacement is computed by considering the different possible failure mechanisms that can be triggered at the local level of the soil-anchor interaction. Six different failure mechanisms are in general possible (modes A, B, C, B1, BY and B2 of Figure 5), depending on the geometry of the problem (thickness of the unstable layer, length and diameter of the anchor) and on the strength parameters of both the soil and the anchor. As it is evident, the limit condition can be reached in the case of full mobilization of soil pressure (modes A, B, or C) or when the maximum bending strength is mobilized in the anchor, with the activation of one or two plastic hinges (modes B1, BY or B2), without mobilizing the shear strength of the anchor along the sliding plane. From this, it is evident that the value of the stabilizing action cannot in any case be assimilated to that of the shear strength of the steel rod constituting the anchor.

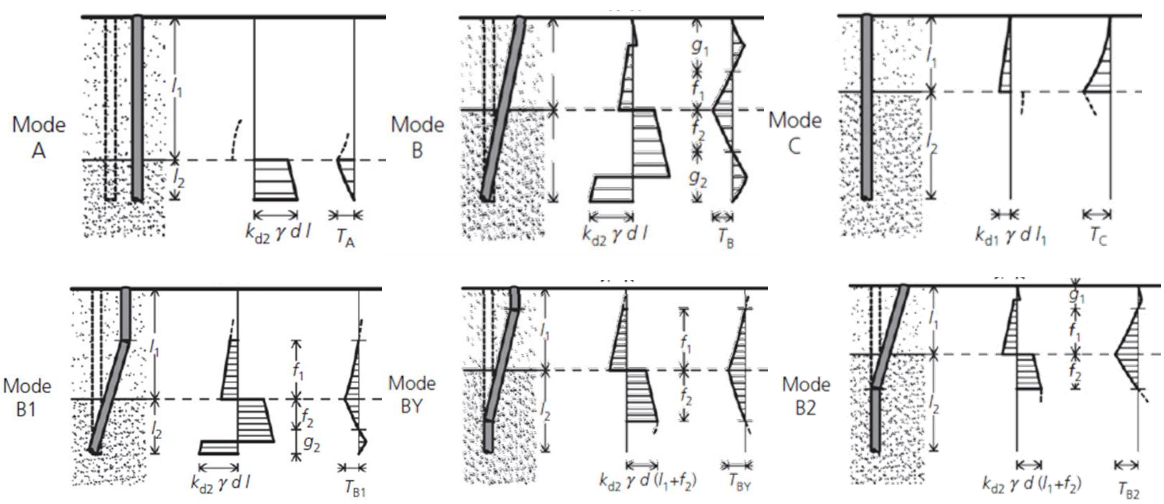


*Figure 5. Failure mechanisms for the soil-anchor system subject to a lateral soil displacement (Di Laora et al., 2017).*

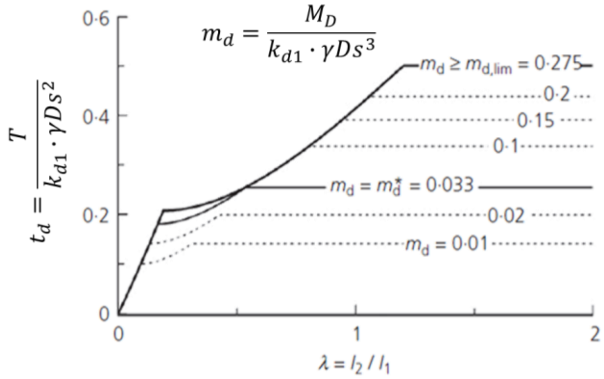


*Figure 6. Values of the dimensionless stabilizing action $t_d$ provided by one single anchor (Di Laora et al., 2017).*

All the six solutions are summarized in the non-dimensional graph at Figure 6 (Di Laora et al.; 2017), where the dimensionless value $t_d$ of the stabilizing action is plotted against increasing values of the dimensionless length $\lambda$ of the anchor. The dimensionless value $t_d$ corresponds to a force $T$, provided by an anchor of diameter $d$, grouted in a hole of diameter $D$ (generally coinciding with the ideal diameter of the grouted section), in a soil layer of unit weight $\gamma$ and thickness $s$. The $\lambda$ parameter expresses the ratio between the anchor length $l_2$ beyond the sliding plane and the thickness of the unstable layer $l_1$=$s$).

The values of $t_d$ are however strictly influenced by the activation of the plastic hinges in the anchor, and, consequently, different curves are plotted in the graph, depending on the value of the dimensionless bending strength $m_d$ (function of the yielding bending moment $M_D$ of the anchor section; the value of the parameter $k_{d1}$ has always been set to 40). It is worth noting that the value $M_D$ does not necessarily correspond with the ultimate strength $M_Y$ of the anchor in pure bending test, but, through the well-known $M - N$ interaction envelope domain for the anchor section (usually, a steel rod); it depends on the value $\mathrm{N_D}$ of the tensile action $\mathrm{N}$ (see Figure 7, where $\mathrm{N_Y}$ represents the ultimate strength in pure tensile tests) mobilized in the anchor by the pressure $q$ developed over each single span of the mesh at the soil-mesh interface. Consequently, the actual stabilizing action $T$ provided by each anchor along the sliding plane can be evaluated only by means of a coupled analysis, accounting for both the bending and the tensile response of the anchor. In other words, the working condition of the mesh also influences the anchor resistance against transverse soil sliding. At each run, the program will solve this coupled problem by numerically determining the pair of values ($M_D, N_D$) lying on the boundary of the $M - N$ interaction domain. Such a condition also represents the safety check for the anchor, at least for the section where a plastic hinge is activated, since a maximum value in the bending moment diagram is thus expected with a nil value of the shear force.

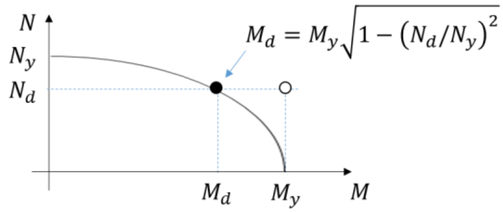


*Figure 7. M-N interaction diagram for an anchor steel section.*

The resulting value of the stabilizing action T, under the hypothesis that no significant interaction arises between neighbouring anchors (i.e. each anchor is independent from the others), is then simply introduced in the slope stability analysis as an additional equivalent cohesive strength acting along the sliding plane of the unstable layer, and uniformly distributed over the area of influence of each anchor.

One last hypothesis assumed in the analyses is the introduction of a second additional term to the "natural" cohesion of the material, linearly decreasing from 3 kPa with the thickness of the unstable soil layer "s" to 0 kPa at a depth of 2.0 m. This term takes into account in a simplified way the local strengthening effect of the soil induced at shallow depths by the roots of the existing vegetation, as well as the increase in the soil strength due to partial saturation (Cazzuffi et al., 2014; Fredlund and Rahardjo, 1993).

As far as seismic analyses are considered, a simple pseudo-static approach has been adopted. The seismic actions are modelled as equivalent static forces along the vertical and horizontal directions, and expressed as a fraction of the total soil weight through the pseudo-static coefficients $k_v$ and$k_h$, respectively (see e.g. Figure 8b and Figure 10b).

This conceptual framework of analyses, is adopted in Mac S-Design to study the stability of a slope and is based on the two approaches presented in detail in the following paragraphs,. The procedure is applied to assess the Factor of Safety both in the actual state, namely a the "pre-intervention" phase, as well as to design the intervention, namely a stability analysis suitable to verify the applied product.

## 3.2 Approach 1

In this approach the stability analysis is run by approximating the sliding surfaces illustrated in Figure 4 by means of two-blocks failure mechanisms along the slope (Figure 8a). Each failure mechanism is composed of a layer of thickness $s$ and length $L$, sliding along the inclined bedrock according to a translational displacement field $U$. The toe of the failure mechanism is composed of a rigid triangular block (points $P'$-$P"$-$Q$), sliding along its base failure plane of a quantity $U_T$, corresponding to a normal displacement component $U_N$ with respect to the slope, over a length $L_a$ (between points $P'$ and $P"$). In the presence of the wire mesh, this length $L_a$ represents the "active" length of the stabilizing system, i.e. the zone of the slope where the stabilizing contact pressure $q$ is mobilized between the mesh and the slope.

The interface between the sliding mass and the toe wedge (segment $P'Q$) is assumed here to be normal to the slope, whilst the inclination of the toe sliding plane (segment $P"Q$) is numerically estimated by an optimizing procedure. This procedure consists of two separate steps (1-2), to be solved for each failure mechanism considered in the slope, and by an optimizing procedure (3):

(1) the equilibrium of the upper sliding block is firstly solved (Figure 8b), by introducing a safety factor $F_S$, reducing its base shear strength $T_L$. The upper boundary condition is represented uniquely by the possible water thrust $U^*$ in the tension cracks. Lower boundary conditions are represented by the interface forces with the active triangular block at the base, i.e. the normal and tangential forces $R'_N$ and $R'_T$, respectively, and by the water thrust $\widetilde{U}$ along the

line $P'Q$. Owing to the displacement compatibility between the upper sliding block and the base triangle, in the case of activation of a failure mechanism, a relative sliding force $U_N$ must be considered along the line $P'Q$.

(2) The equilibrium of the triangular block $P'$-$P"$-$Q$ is then imposed (Figure 8c), by considering again a failure condition along its base ($P"$-$Q$) between forces $T_{L,a}$ and $N'_a$, and introducing the possible water base thrust $U_{w,a}$. The corresponding value of the pressure $q$ over the active length $L_a$ can then be derived.

(3) The obtained value of $q$ is then maximized with respect to the inclination $\beta$ of the line $P"$-$Q$, thus finding the most probable failure inclination for the active base triangle, and the corresponding active length $L_a$.

The numerical procedure is represented in Figure 9.

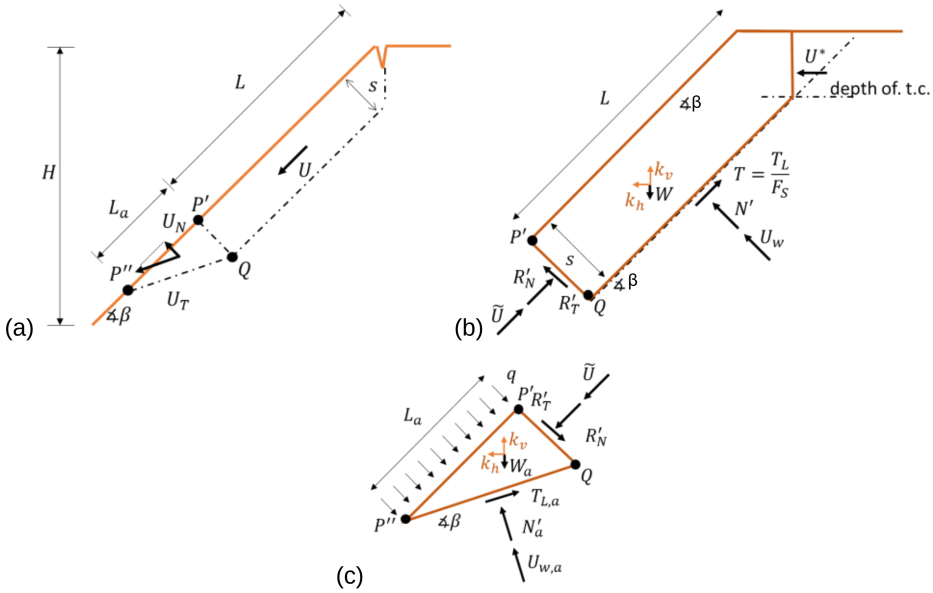


*Figure 8. (a) simplified two-blocs failure mechanisms adopted in the approach 1.*

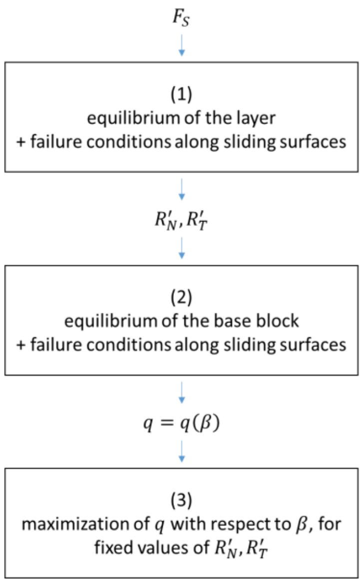


*Figure 9. Flow chart of the solving procedure for the approach 1.*

## 3.3 Approach 2

In this approach, ideally more suitable for gentle slopes, two-block failure mechanisms are again defined in the slope, but a different lower boundary condition is adopted for the sliding layer. The base active triangle $P'$-$P"$-$Q$ is now assumed to slide horizontally (failure plane $P"$-$Q$ is horizontal) and with a vertical interface between the upper sliding layer and the triangle (segment $P'Q$ is vertical; Figure 10a). Under these assumptions, the state of stress at failure along the interface $P'Q$ can be computed without the need of a numerical optimization procedure and expressed as a function of a generalized passive earth pressure coefficient $K_P^*$ (Lancellotta, 2012). The resulting maximum supporting force $R$ provided by the base active triangle coincides with its passive resistance, and it can be analytically expressed as:

$$R = \frac{1}{2}\gamma'_{eq}\left(\frac{s}{cos\,\alpha}\right)^2 K_p^* + 2\frac{c's}{cos\,\alpha}\sqrt{K_p^*} + \frac{qs}{(cos\,\alpha)^2}K_p^* + q\cdot\tan\alpha\cdot L_a. \qquad (3)$$

In equation (3), $\gamma$ is the unit weight of the soil and, in order to properly introduce the passive earth pressure coefficient, the normal contact pressure $q$ mobilized between the soil and the mesh has been split into two separate components, the vertical- and the tangential respectively.

The solving procedure can be ideally represented as in the flow chart in Figure 10c.

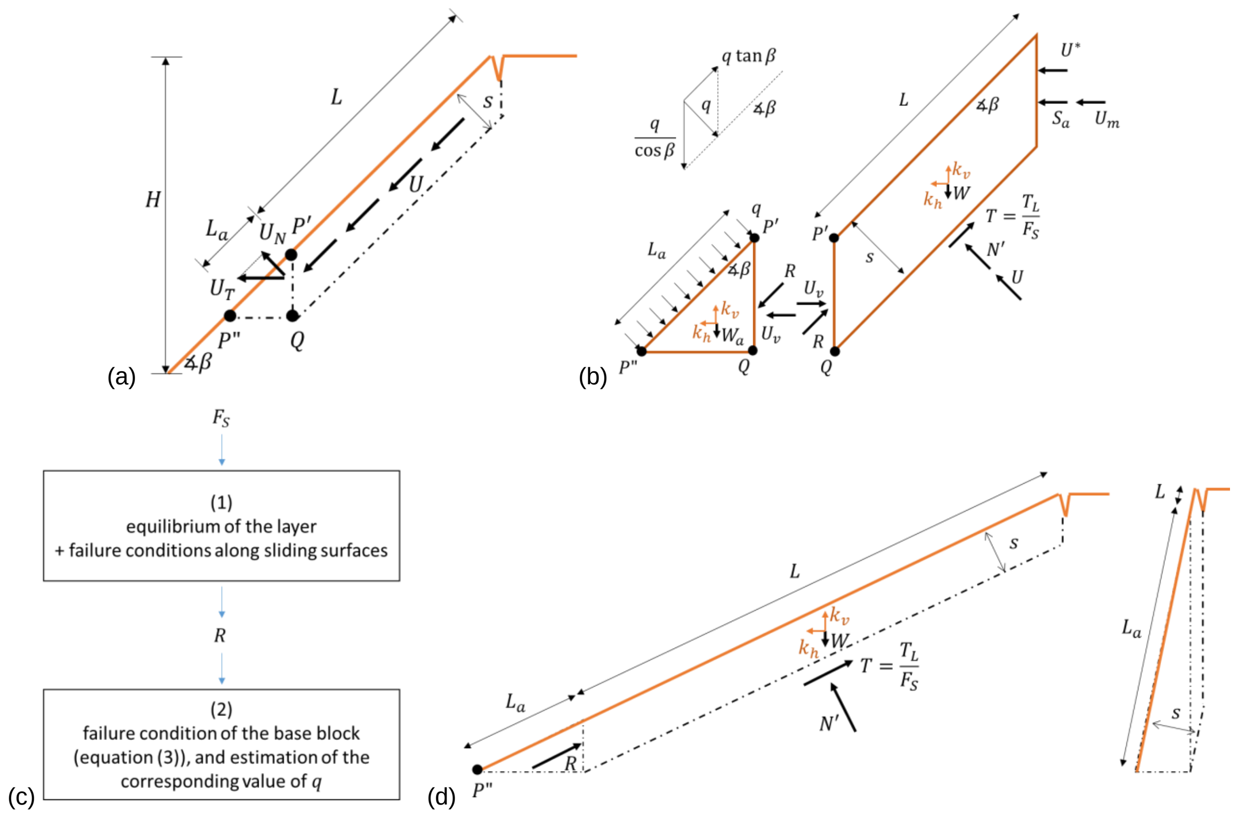


*Figure 10. Approach 2: (a) assumed failure mechanism; (b) equilibrium of the two blocks; (c) flow chart of the solving procedure; (d) example of gentle and steep slope.*

This approach may however, be largely inaccurate in the case of very steep slopes (Figure 10d), since the base triangle would become the dominant term in the equations, thus rendering meaningless, the computation of a safety factor for a soil layer of very limited length $L$. In order to prevent such a condition, a limitation on the acceptable value of the ratio $s/H$ is introduced in within Mac S-Design.

Furthermore, the estimation of the passive earth pressure coefficient $K_P^*$ can only rigorously be obtained for slope angle $\beta$ smaller than the soil friction angle $\phi'$.

## 3.4 Results of the pre-analysis

The combined use of these two approaches of analysis is adopted in a first stage to assess the stability of the unstable surficial layer of a slope before the intervention, i.e. without any stabilizing mesh ("pre-analysis" phase). As in the case of the stability analyses with the mesh, Mac S-Design runs both approaches (Figure 8, Figure 10) in order to assess the slope stability condition before proceeding to the second phase. In the pre-analysis, the stabilizing pressure "q", provided by the mesh, is assumed to be nil; the product has not yet been installed. This procedure enables the minimum pre-analysis Factor of Safety ($FS_0$) to be evaluated for the unstable surficial layer of the slope.

In this stage of pre-analysis, the User can run parametric analyses both to investigate the sensitivity of the input parameters and to assess their critical combination related to a Factor of

Safety $FS_0$. The pre-analysis is important in order to assess the potential instability of the surficial soil layer as an initial step of the subsequent stability analyses (§3.5). Having a preliminary assessment of the stability can also lead the User to the selection of the more appropriate product for the intervention.

## 3.5 Results of the stability analyses

The results of the stability analyses for a prescribed $F_S$ value is generally expressed as an envelope of the values of the mobilized pressure $q$ along the active length $L_a$, for each considered failure mechanism in the surficial layer and for the two adopted stability analysis approaches. If the values of $q$ are plotted against the elevation $z$ of each mechanism, the resulting curve (red curve in Figure 11) represents the profile of the computed pressure distribution for a fixed value of safety factor $F_S$. It is worth noting that this curve does not represent the expected pressure distribution in service conditions for the stabilizing system, but only the envelope of the possible pressure values, corresponding with the imposed $F_S$ value.

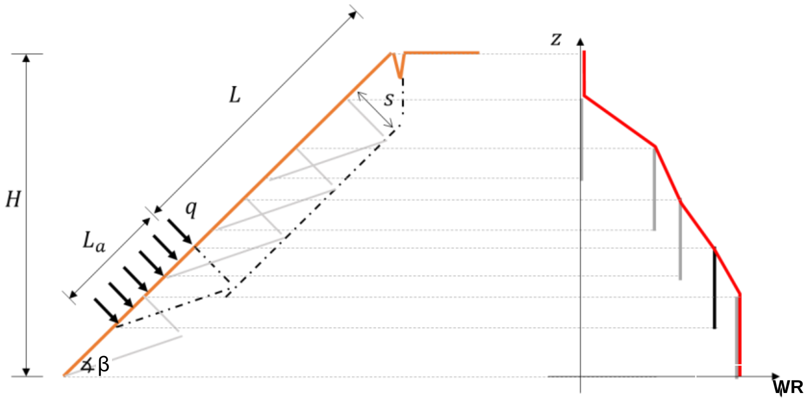


*Figure 11. Envelope of the required contact pressure distribution along the slope.*

As previously pointed out in §3.1, the program output also provides the values of the tensile actions in the anchors, corresponding with the computed distribution of the pressure $q$, having already checked, as a result of the coupled analysis, the working condition $(M_D, N_D)$ in the $M - N$ interaction domain for the sections where plastic hinges are activated. This pressure $q$ then allows a meaningful working ratio parameter to be introduced in order to easily check the behaviour of the mesh. This output parameter is expressed as a percentage (%) and this indicates the maximum ratio under which the mesh performs compared to its capacity. The verification on the mesh is satisfied when the working ratio does not exceed 100%.

# 4 Characteristic Functions

Following the definition of equation (2), for each considered failure mechanism, the characteristic function represents the relationship between the "far field" soil displacement $\boldsymbol{U}$ (i.e., the soil displacement for the considered failure mechanism) and the mobilized stabilizing action at the soil-structure interface:

$$A^F = A^F(\boldsymbol{U}), \tag{4}$$

(subscript "k" is here omitted for the sake of brevity). In general cases, the displacement $\boldsymbol{U}$ is actually represented by an entire soil profile, so that equation (4) is of vectorial nature.

In the specific case of anchored wire meshes and sliding failure mechanisms, however, the stabilizing action is represented by the distributed pressure $q$, whilst the far field displacement corresponds with the normal component $U_N$ (with respect to the slope profile) of the total displacement $U_T$ of the active block $P'$-$P"$-$Q$, so that a scalar function

$$q = q(U_N), \tag{5}$$

called "characteristic curve", can simply be adopted to describe the entire interaction problem.

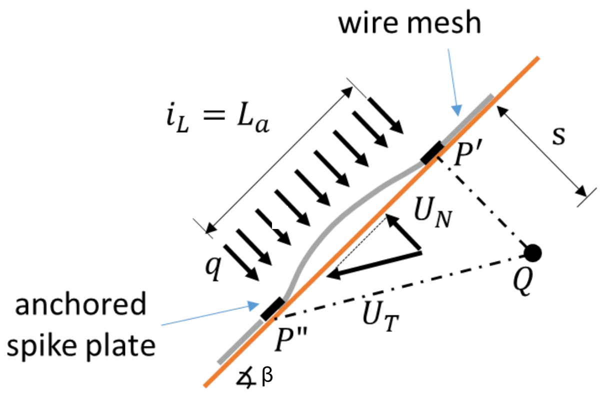


*Figure 12. Qualitative deformed shape of a span of an anchored wire mesh, subject to a soil displacement $U_N$ and developing an average stabilizing pressure $q$ over its active length $L_a$.*

In Figure 12 the ideal case of an active block $P'$-$P"$-$Q$ interacting with a single span of an anchored wire mesh is illustrated, with the underlying hypothesis that the active length $L_a$ of the failure mechanism coincides with the longitudinal spacing $i_L$ of the anchored spike plates along the slope (a specific reduction factor is then introduced on the characteristic curve for the case $L_a < i_L$).

## 4.1 What a Characteristic Curve is

A characteristic curve conceptually represents the relationship between the average value of the contact pressure $q$ mobilized between the soil and the mesh over a span of the mesh and the corresponding normal movement of the backfill soil material. Obviously, at each time the mobilized tensile action in an anchor can be evaluated by simply integrating the pressure $q$ over the area of influence of the anchor (i.e. the square of the anchor spacing $i_L$). This entire curve is fundamentally dependent on the mechanical characteristics of both the soil and the mesh used to retain the unstable backfill soil in the case of a real application.

A slope reinforced with a surface stabilisation mesh can be then schematically considered as a series of nails loaded by the pressure $q$ transferred through the relevant influence area of the mesh. Following the aforementioned sub-structuring approach, each single anchor (assumed to be independent from the others, since high values of the diameter-to-spacing ratios are generally adopted in practice) can be singularly investigated as an simple “macro” element to analyse the actual stresses acting on its relevant components, i.e. steel mesh, anchor and soil. A scheme of a 3D finite element model representing ¼ of a span of mesh with its underlying soil is presented in Figure 13a, where a soil volume of dimensions $i_L \times i_L \times s$ is considered, together with a membrane reproducing the behaviour of the wire mesh and a rigid anchor plate.

Such a numerical model was used to carry out 3D elastoplastic finite element analyses, by considering a large displacement computational scheme, in order to accurately capture the membrane behaviour of each wire mesh product, that is in fact capable of providing tensile actions only upon relevant transversal displacements (i.e. out-of-plane, normal to the slope). The simulation is run by fixing the position of all the nodes corresponding to the plate, and by imposing a uniform displacement $U_N$ to the lower boundary of the soil volume (i.e. a far field displacement). For the sake of simplicity, only one quarter of the soil volume was numerically reproduced, and, because of symmetry, smooth boundary conditions are imposed on all the vertical boundaries, with no normal displacement. An example of the soil displacement contours observed in the entire soil volume is shown in Figure 13b, for a test run until an imposed base displacement $U_N$=20cm.

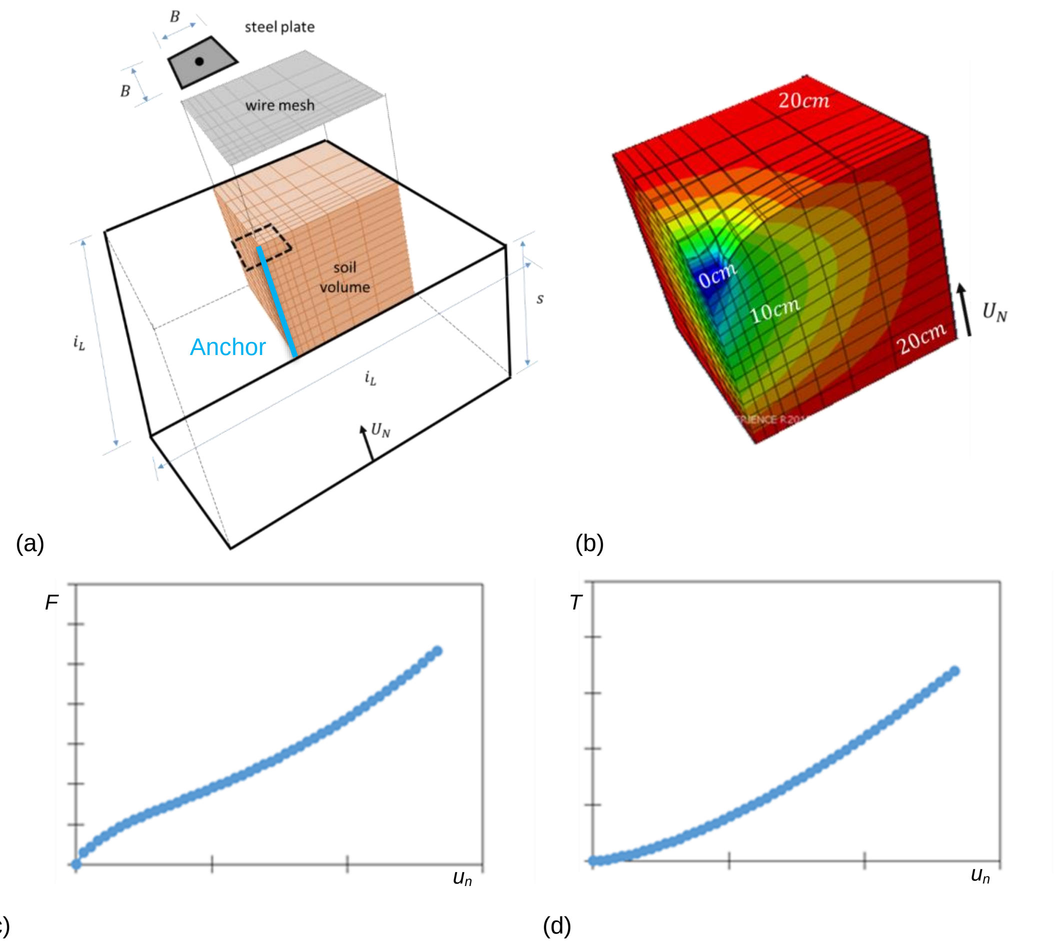


*Figure 13. Numerical simulation of the elementary element: (a) 3D numerical model; (b) contour of soil displacement profile for a base displacement $U_N$; (c) example of characteristic curve; (d) evolution of the maximum tensile force in the mesh during loading.*

Numerical simulations are obtained by assuming (i) the soil behaves as an elastic perfectly plastic medium, with a Mohr-Coulomb failure criterion and non-associate flow rule, and (ii) the wire mesh can be assimilated to an equivalent homogeneous and isotropic elastic membrane.

The results of the simulations are expressed in terms of the load-displacement curve $F - U_N$ (Figure 13c), where *F* represents the tensile force acting on the nail, and of the tension-displacement curve $T - U_N$ (Figure 13d), where *T* represents the maximum tensile action developed in the mesh during the loading process. Capturing the initiation of this phenomenon (depending both on the mechanical parameters of the considered mesh and on the soil characteristics) is then of fundamental importance to define the failure condition on the $F - U_N$ curve, representing the required “characteristic curve”. An example of characteristic curves for different meshes is shown in Figure 14.

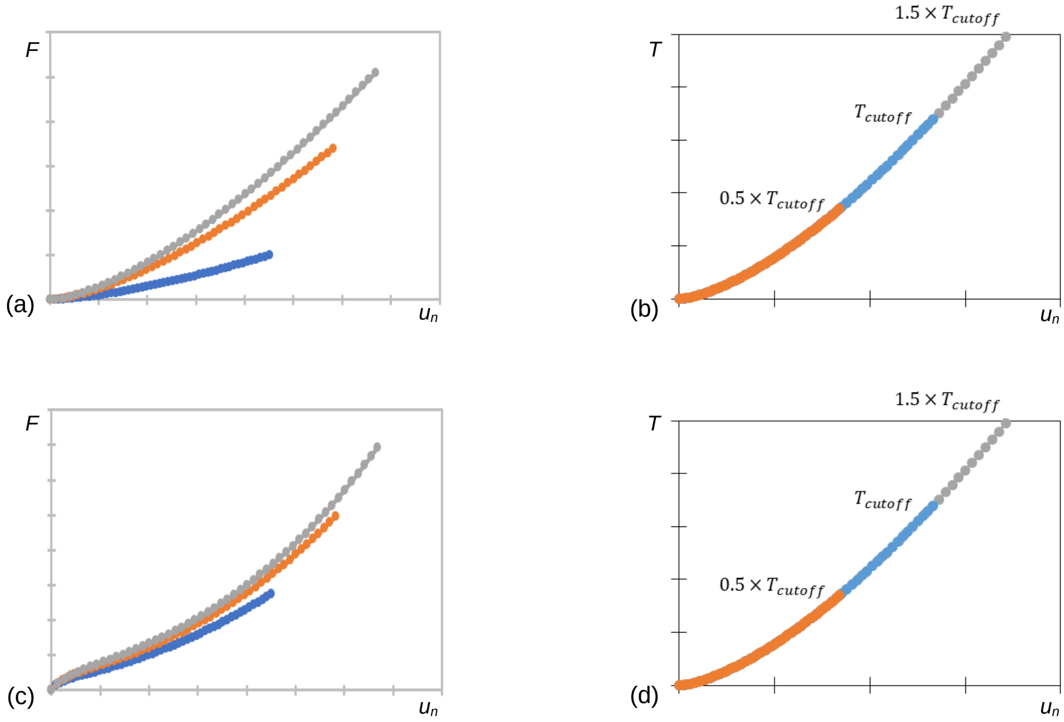


*Figure 14. Examples of $F$ and $T$ curves on meshes with different stiffness and strength values (a, c) and on meshes with the same stiffness and increasing strength values (b, d).*

The governing parameters of the process are then defined by:

- the mechanical properties of the soil (unit weight, $\gamma$, friction angle, $\phi$, cohesion, $c$, dilation angle, $\psi$, Young modulus, $E$, and Poisson coefficient, $\upsilon$),
- the geometry of the system (anchor spacing, $i_L$, average plate dimension, $B$, mesh thickness, $t$),
- the mechanical properties of the mesh in tensile tests (stiffness, $J$, strength, $T_{cutoff}$).

## 4.2 How Characteristic Curves are derived

The numerical model briefly described in the previous paragraph has been extensively adopted to run numerous 3D finite element simulations, thus exploring the influence of the above cited governing parameters on the characteristic curves. From a phenomenological point of view, the system shown in Figure 13a can be assimilated to an equivalent 1D rheological element, composed of the steel plate and the wire mesh, working in parallel against the underlying soil. The behaviour of each one of these two elements is highly nonlinear. In particular, the steel plate is assumed to behave as a rigid isolated shallow foundation on a soil deposit, whose load settlement curve is characterized by a progressive reduction of the stiffness, until its bearing capacity $F_{lim}$ is reached. The membrane response, owing to its large displacement, is instead characterized by an important stiffening effect (Figure 15).

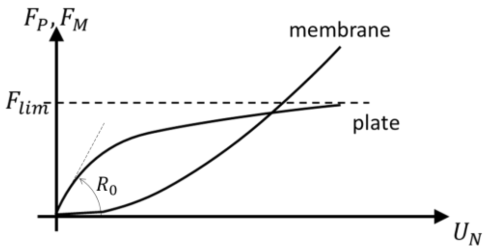


*Figure 15. Ideal behaviour of a plate and of a membrane in punching tests.*

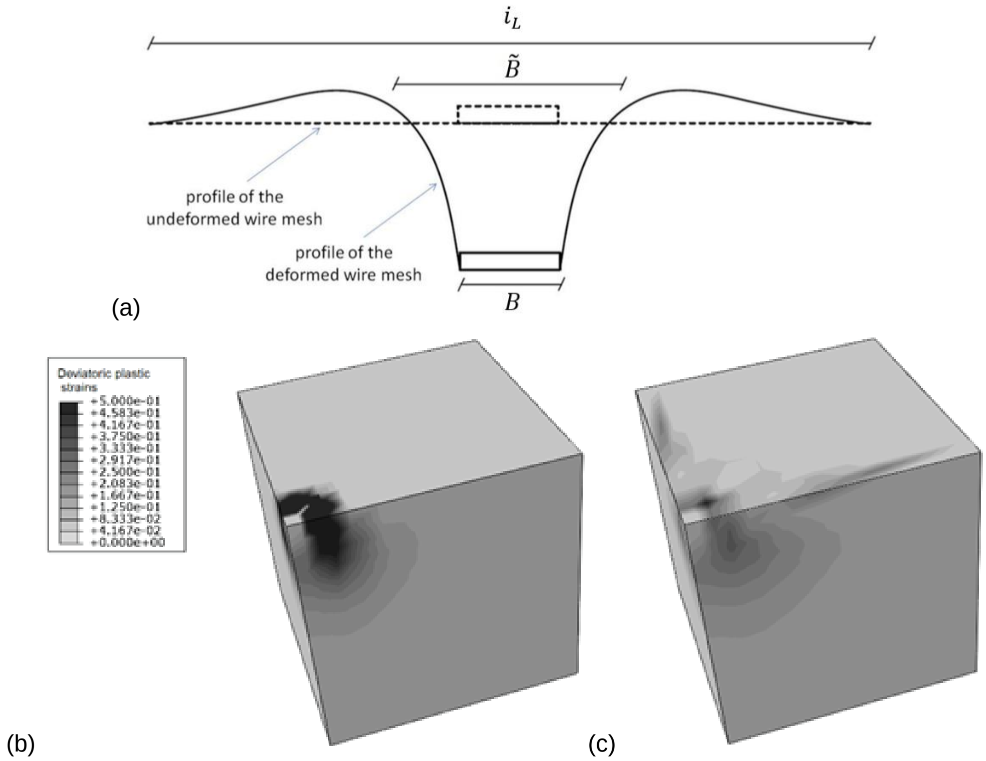


*Figure 16. (a) schematic view of the "widening" effect induced by the wire mesh. Comparison of plastic strains: (b) test with the plate only and (c) test with plate + mesh.*

The membrane, however, actually works by redistributing the vertical stresses over a wider area $\tilde{B}$ with respect to the actual average size $B$ of the plate (Figure 16a), thus increasing the local confinement and reducing the strain concentration into the soil (Figure 16b and c). The behaviour of the two elements, namely the membrane and the plate, is then coupled, and this effect can be modelled by considering a progressive increase in the plate bearing capacity $F_{lim}$ induced by the membrane.

In accordance with the well-known expression proposed by Butterfield (1980), the load-settlement curve of an isolated foundation subject to a vertical centred load can in fact be expressed as:

$$F_P = F_{lim} \cdot \left[1 - exp\left(-\frac{R_0 \cdot U_N}{F_{lim}}\right)\right], \tag{7}$$

where $R_0$ is its initial elastic-plastic stiffness and $F_{lim}$ is its ultimate bearing capacity. A square foundation of size $\tilde{B}$, $F_{lim}$ is usually computed by means of the Brinch-Hansen formula (1970):

$$F_{lim} = \tilde{B}^2 \cdot \left(\frac{1}{2} \cdot \gamma \cdot \tilde{B} \cdot N_\gamma \cdot s_\gamma + c \cdot N_c \cdot s_c\right), \tag{8}$$

with:

- $\gamma$ and $c$ representing soil weight and cohesion, respectively;
- $N_\gamma$ and $N_c$ representing the bearing capacity factors for shallow foundations (depending on soil friction angle uniquely);
- $s_\gamma$ and $s_c$ representing shape factors for squared foundations.

The aforementioned "widening" effect induced by the wire mesh then has a direct effect on the size $\tilde{B}$ of the equivalent foundation of equation (8), defined as:

$$\tilde{B} = B + \Delta B(U_N), \tag{9}$$

where the actual average size $B$ is progressively increased by a quantity $\Delta B(U_N)$. This latter term evolves together with the plate settlement and strictly depends on both the soil and the mesh mechanical properties. A second indirect effect on $F_{lim}$ is also present, since the increase in the equivalent size $\tilde{B}$ with respect to the anchor spacing $i_L$ progressively transforms the system into an ideal "macro" oedometer, whose bearing capacity $F_{lim}$ tends to infinite. Such an effect is modelled by defining the bearing capacity factors of equation (8) as a function of the ratio $i_L/\tilde{B}$:

$$N_\gamma = N_\gamma\left(i_L/\tilde{B}\right) \text{ and } N_c = N_c\left(i_L/\tilde{B}\right). \tag{10}$$

Owing to such highly nonlinear and coupled behaviours, the numerical description of the mechanical response of the entire system can be obtained only in an incremental way, as formally expressed by the following equation:

$$\dot{F} = \dot{F}_P + \dot{F}_M + \dot{F}_{PM} = (K_P + K_M + K_{PM}) \cdot \dot{U}_N. \tag{12}$$

In equation (12) dots stand for increments, $K_P$ and $K_M$ represent the local tangent stiffnesses to the curves represented in Figure 15, and $K_{PM}$ is the coupling stiffness, governed by the terms of equations (9) and (10). The coupling stiffness, in particular, is dependent on the relative soil-membrane stiffness $J/(E \cdot t)$, on the anchor spacing $i_L$, on average plate dimension $B$, and its evolution was calibrated on the above discussed 3D FEM analyses, by defining the aforementioned functions $\Delta B(U_N)$, $N_\gamma(i_L/\tilde{B})$ and $N_c(i_L/\tilde{B})$.

Finally, as was previously cited, it is worth remembering that the characteristic curves are derived by assuming a linear elastic and isotropic behaviour of the membrane, and the failure condition is reached in the characteristic curve when the tensile force $T$ in the membrane reaches its limit cut-off value $T_{cutoff}$. Once the equation (12) is numerically integrated by means of an ad hoc explicit numerical subroutine, the curve $F = F(U_N)$ is finally obtained. Such a curve is then normalized by the real area of influence of each anchor, represented by the product $i_L \times i_L$, in order to derive the curve $q = q(U_N)$ to be introduced in the hybrid method for the slope stability analysis.

As it was previously mentioned, this numerical procedure has been calibrated in the ideal case of $L_a \geq i_L$, i.e. in the case that the thickness $s$ of the unstable layer generates a failure mechanism with an active length $L_a$ equal or larger than the anchor spacing $i_L$ (the whole span of mesh is then influenced by the soil displacement $U_N$, as in Figure 17a). When, on the contrary, the active length

$L_a$ is lower than the anchor spacing $i_L$ (as happens for thin layers of unstable material; Figure 17b), only a reduced part of the mesh span is influenced by the soil displacement $U_N$, and the efficiency of the system is reduced. Such a geometrical effect is modelled by introducing a correction factor on the characteristic curve, reducing the value of $q$ whenever $L_a < i_L$.

The final expression can then be formally written as:

$$q(U_N) = F(U_N) \cdot \frac{\min(1, L_a/i_L)}{i_L \times i_L}. \tag{13}$$

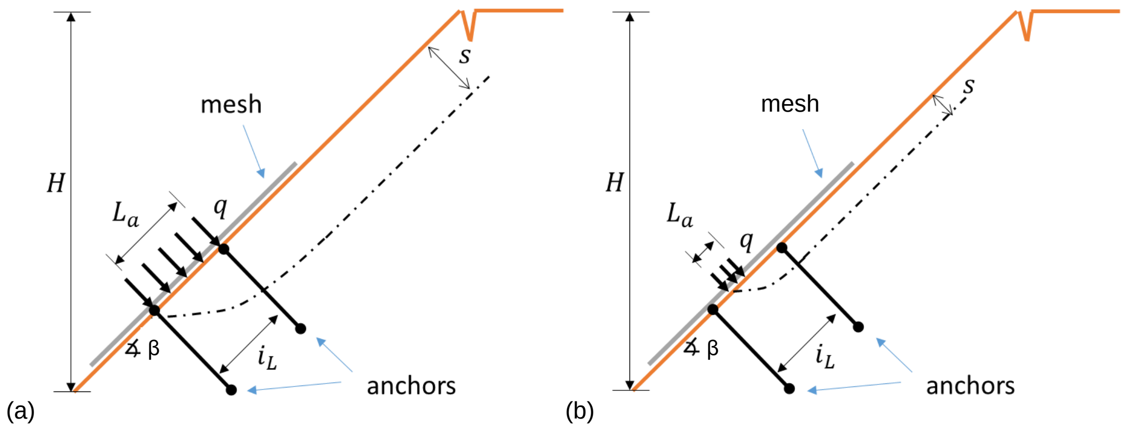


*Figure 17. Effect of the thickness $s$ on the soil-mesh interaction: (a) case of active length $L_a$ coinciding with the anchor spacing $i_L$ and (b) case of $L_a < i_L$.*

## 4.3 How the Characteristic Curves are employed

The characteristic curves represented by equation (13), computed for each adopted failure mechanism in the slope, are then employed to check the working condition of the mesh, i.e. if the envelope of the required contact pressure distribution (shown in Figure 11) can be sustained by the mesh. A meaningful working ratio parameter has been introduced in order to easily check this point. A calculation example is given in §9 to further clarify its application.

# 5 Nail Design

Mac S-Design also includes an additional tool devoted to nail design. The goal of this tool is to help the designer both to define the drilling length and to carry out a local verification of the chosen steel section. The reference model is shown in Figure 18.

Coherent with the approach of Mac S-Design, the forces considered in this design approach for the nails are those derived from the stability analysis of the unstable surficial layer. An analysis of the forces acting on the anchors due to the global stability must be calculated with a tool specifically designed for this purpose.

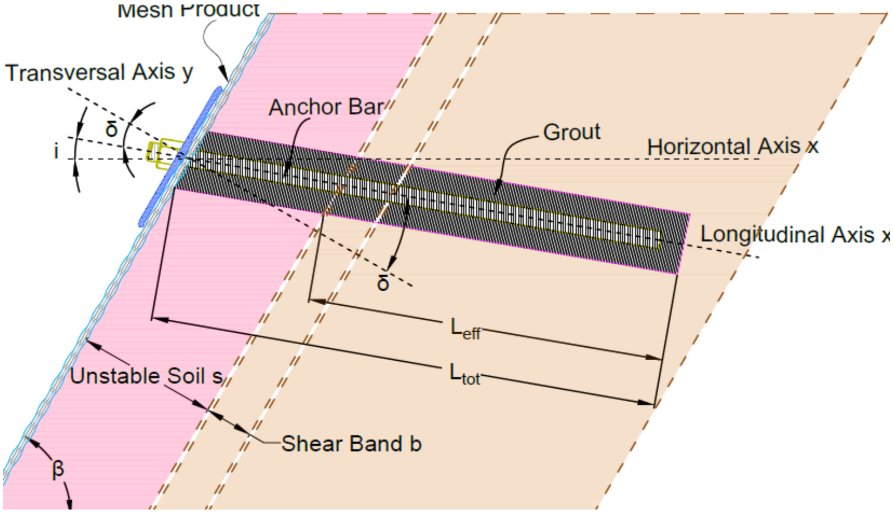


*Figure 18. Scheme of the relevant geometrical nail parameters.*

Where the main parameters are:

- *s* as the thickness of the unstable layer,
- *b* as the thickness of the shear band,
- $\delta$ as the angle between the anchor and the perpendicular to the slope,
- *i* as the inclination of the nail to the horizontal.

To properly dimension the anchors, the geotechnical parameters of the soil as well as the bond stress between the soil and the grout should be known.

Two main analyses are then carried out on the anchors as  presented in the following sections. On one hand the definition of the required drilling length is computed, on the other hand, the steel section in then verified in the M-N domain.

## 5.1 Drilling Length - Design approach

To determine the anchor length, the design approach is the same as Bustamante & Doix (1985), considering the nail as a loaded element at the head. The total length of the nail will be defined as follow:

$$L_{tot} = L_{s,inst} + L_{shear} + L_{anch} \tag{14}$$

where:

- $L_{tot}$ is the Total Length of the nail,
- $L_{s,inst}$ is the thickness of the unstable layer in the direction of the nail,
- $L_{shear}$ is the thickness of the shear band in the direction of the nail,
- $L_{anc}$ is the Effective Length of the nail,

while $L_{inst}$ and $L_{shear}$ are known quantities, defined by the geometry and the depth of the unstable layer while the $L_{anch}$ must be calculated.

As a consequence, given the acting pull-out force and defining the bar type and diameter, it is possible to check if the chosen solution is able to transfer the load applied from the mesh into the stable layer. The most general version of the Bustamante – Doix approach is usually given by the following equation:

$$F_{act} \cdot \gamma_F = \pi \cdot d \cdot \alpha_d \cdot L_{anc} \cdot \frac{\tau_{bond,d}}{\gamma_b} \tag{15}$$

where:

- $F_{act}$ is the acting force along the nail,
- $d$ is the drilling diameter,
- $L_{anc}$ is the unknown, the Effective length of the nail,
- $\tau_{bond,d}$ is the design bond stress between the grout and the soil,
- $\alpha_d$ is a correction factor for the drilling diameter (or radius),
- $\gamma_f$ is an amplifying factor,
- $\gamma_b$ is the safety factor on the soil-grout adhesion.

Partial safety factors are applied to the acting force $F$ and to the bond stress $\tau_{bond}$, to consider the possible errors in the definition of these parameters or variation in the values. Using the (15) the Effective Length of the nail $L_{anc}$ can be defined, as:

$$L_{anc} = \frac{F_{act} \cdot cos\,(\delta)}{\pi \cdot d \cdot \alpha_d \cdot \tau_{bond}} \tag{17}$$

where:

- $F_{act}$ is the acting pull-out force on the anchor,
- $F$ is the force, perpendicular to the slope face, delivered by the mesh,
- $\delta$ is the angle between the perpendicular to the slope and the anchor.

The total drilling length will be defined as for (14).

## 5.2 Steel section check

The safety check on the $M - N$ diagram for the sections where plastic hinges are activated, is an internal part of the coupled stability analysis, as already pointed out (see §3.1). The solution provided by the program then automatically respects this limit condition (no shear force is considered, since in a plastic hinge a peak value of the bending moment can be generally assumed).

Other more detailed structural safety checks along the anchor, if needed, would in principle require the definition of the distribution of internal actions along the whole anchor axis.

Furthermore, Mac S-Design also allows both the tensile and the shear verifications to be carried out. The shear verification is provided on the sliding plane of the unstable surface.

## 5.3 Plate connection

The characteristic curves, as described in (§4), consider the cut-off value depending on the strength of the product considered in the design phase. The plate is simply assumed to be a rigid body, with stiffness and strength values sufficiently high to prevent its failure. Further and more detailed verifications can be carried out separately by the User.

# 6 Definition of the mechanical parameters

The stability analysis provided by Mac S-Design is primarily dependent on the use of the characteristic curves as a soil-mesh interaction system (see §4). In this light, the results achieved are dependent on both mechanical parameters of the soil and of the selected product.

## 6.1 Geotechnical Soil Parameters

The governing geotechnical soil parameters, beyond the soil unit weight, are those generally defined for a linear elastic–perfectly plastic material, with a Mohr-Coulomb failure criterion and non-associate flow rule. This implies in general the calibration of five constitutive parameters:

- soil friction angle $\phi'$
- soil cohesion, $c'$
- soil dilation angle, $\psi$
- soil Young modulus, $E$
- soil Poisson coefficient, $\upsilon$

Despite Mac S-Design is of general validity and any meaningful combination of such parameters can in principle be treated, a simplified input procedure has been adopted. The values of the soil friction angle and of the soil cohesion can be assigned directly on the basis of the available soil characterization (acceptable ranges of values are specified in the User's Manual). The soil dilation angle and the soil Young modulus are calibrated according to the definition of two general types of materials (granular, e.g. sand or silt; or cohesive, e.g. fine silt or clay) and two compaction states (i.e. loose/soft or dense/compacted). This will then give rise to a double entry classification, with four general types of combinations. The soil Poisson coefficient is instead fixed, for the sake of simplicity, to 0.3.

The values of the Young modulus are computed in accordance with the well-known formula proposed by Janbu (1963):

$$E = K \cdot p_a \cdot \left(\frac{\sigma_h}{p_a}\right)^n \qquad (18)$$

where $p_a = 101{,}325kPa$ is the atmospheric pressure. A representative value of the effective horizontal stress $\sigma_h$ is computed at a reference depth corresponding with the average plate dimension $B$, by assuming an at-rest earth pressure coefficient $K_0 = 1 - sin\ \phi'$. By adopting the aforementioned double entry classification, and in accordance with Janbu (1963), Lade and Nelson (1987) and Hoffman (2016), the value of the parameter $n$ in equation (18) can be defined as in the following table:

| | sand/silt | silt/clay |
|---|---|---|
| **loose/soft** *(void ratio more than 40%)* | $n$=0,8 | $n$=0,9 |
| **dense/mid hard** *(void ratio up to 40%)* | $n$=0,2 | $n$=0,5 |

whilst the coefficient $K$ can be estimated as 100x the passive earth pressure coefficient $K_P$ for the considered soil.

Finally, the value of the soil dilation angle has been assumed to be a function of the soil friction angle and the degree of compaction. In particular, for dense materials $\psi$ is assumed to vary between $\phi'/5$ and $\phi'/2$ for increasing value of the soil friction angle, whilst for loose materials $\psi$ is varies between $\phi'/10$ and $\phi'/4$.

## 6.2 Mechanical parameters of the product

The mechanical parameters related to each product and concurring to the definition of the specific characteristic curve (that is also related to the specific soil typology (§6.1)), are tensile strength and tensile stiffness. For a complete proper evaluation of the characteristic curve and thus of the overall behaviour, its mechanical properties are considered,.

In this light, the products with a similar resistance in both directions enables much higher cut-off values compared to those products with a large difference between the strength in the two main directions.

Similarly, the stiffness of the product influences the creation of the characteristic curve. A higher stiffness value logically enables a higher stabilizing pressure “q” to be transferred to the retained backfill material for a same reference soil displacement. A reduction factor equal to 1.5 is assumed for the stiffness value used in the calculation.

# 7 Application limits of the approach

The approach presented for rapid preliminary dimensioning of anchored wire mesh systems has been developed by applying a hybrid method to the stability analysis of translational failure mechanisms on ideally infinite soil slopes, once convenient boundary conditions for the sliding layer are introduced, in order to adapt the approach to slopes of finite height. All analyses that move away from the condition of translational failure mechanisms, even if numerically feasible, may be inaccurate. The three main application limits of the current approach are related to (i) geometrical, (ii) mechanical and (iii) theoretical aspects:

(i) More accurate results for failure mechanisms involving the upper part of the slope could be obtained by adopting failure mechanisms other than the adopted translational one, e.g. a rotational mechanism. Similarly, all possible generalized failure mechanisms involving the base of the slope are neglected (Figure 19a). In the case of very steep (subvertical) slopes on cohesive materials, all possible toppling mechanisms are also neglected (Figure 19b) as well complex and composite failure mechanisms potentially triggered for relatively high values of the thickness $s$ with respect to the slope height $H$ (Figure 19c). For these specific mechanisms, ad hoc LEM analyses, run using software capable of taking into account such geometries, are required.

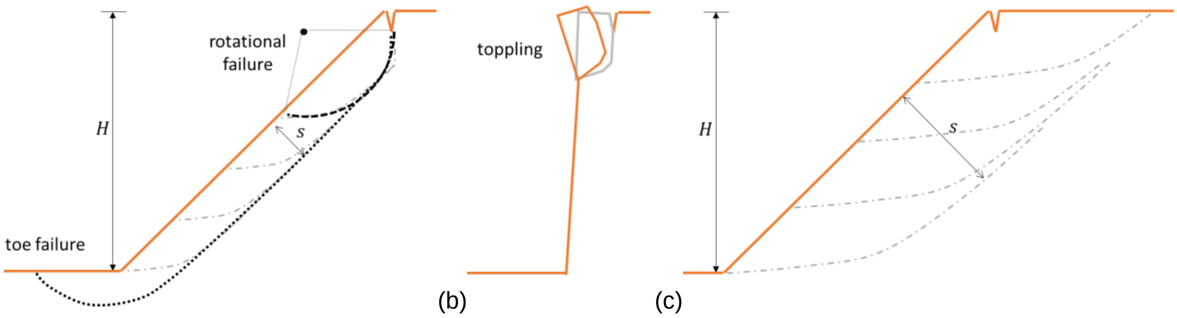


(a) (b) (c)

*Figure 19. (a) rotational and toe failure mechanisms; (b) toppling failure for sub-vertical slopes; (c) composite mechanisms for high thickness of the unstable layer.*

The limits included in Mac S-Design for this parameter (s) have been studied in conjunction with the slope height (H):

**Lower bound, s ≥ 0.5 m**: The lower limit for the thickness of the unstable soil layer has been set to 0.5 m. Input values lower than this lower bound are automatically set to s=0.5 m.

**Upper bound, s ≤ H/5**: The upper limit for the thickness of the unstable soil layer has been set to H/5 m. Input values higher than this upper bound are automatically set to s=H/5.

(ii) The method has been developed under the hypothesis that the wire mesh interacts with a homogeneous, granular or weakly cemented soil. Rocky slopes and rock masses cannot in any case be analysed, and site-specific analyses are required for such cases.

Figure 20. Example of a rocky slope.

(iii) The hybrid methods have been conceived with the aim of providing a meaningful estimation of the mobilized stabilizing force in the slope for an assigned safety level. No time evolution of the equilibrium condition of the slope can be thus simulated. Moreover, in accordance with the definition of “prevention” intervention, it is worth remembering here that the program does not take into account large displacements of the unstable layer, inducing significant changes in the overall geometry of the slope (e.g. as it is sketched in Figure 21, where the accumulation of the failed material deriving from a thin weak layer causes large deformation in the mesh). These are in fact associated with a post-failure condition of the unstable layer, and the mesh in these cases should then be conceived as a protection system, rather than a prevention system, by adopting completely different theoretical and numerical approaches.

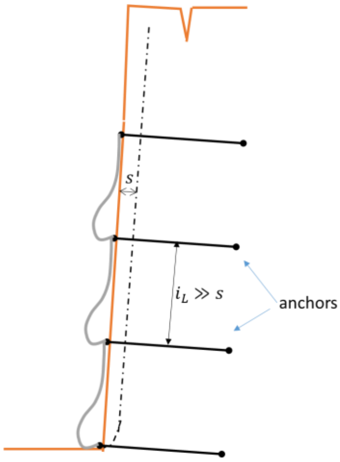


Figure 21. Example of protection system against the failure of a thin weak rock layer on a steep slope.

# 8 Environmental aggressiveness

The environmental exposure is an important factor when designing slope and rockfall protection systems. The description of the site environment and all the geomorphological aspects that this entails, is of crucial importance during the preliminary phase. This section, briefly provides some Standards in according with which, the design procedure is followed. The British Standard BS EN 10223-3:1998, whose main superseded version is the European Standard EN 10223-3:2013, refers principally to “Steel wire and wire products for fencing and netting: Hexagonal steel wire mesh products for civil engineering purposes”.

The definition of the main wire coating requirements are the principle factors for a preliminary configuration of the steel wire mesh to be selected in the solution. For this reason, BS EN 10223-3:2013, Annex A, Table A.1 related to the “Description of environment of installation site, coating wire requirement of Annex A” is provided below. The designer should consider the aspects above in order to better-define the coating requirements to be used on the project.

**Description of environment of installation site, coating wire requirements, EN 10223-3:2013, Annex A**

| Site Environmental level (in accordance with EN ISO 9223:2012, Table 1) | Plastic coating material | Coating | Class EN 10244-2 | Assumed working life of the product (year) |
|---|---|---|---|---|
| **Low Aggressive: (C2)**<br>**Dry conditions**<br>Temperate zone, atmospheric environment with low pollution, e.g. rural areas, small towns (over 100 m above sea level). Dry or cold zone, atmospheric environment with short time of wetness, e.g. deserts, sub-arctic areas | - | Zinc | A | 25 |
| | - | Zn95%/Al5% alloy | A | >50 |
| | - | Zn90%/Al10% alloy | A | >120 |
| **Medium aggressive: (C3)**<br>**Dry conditions**<br>Temperate zone, atmospheric environment with medium pollution or some effect of chlorides, e.g. urban areas, coastal areas with low deposition of chlorides e.g. subtropical and tropical zone, atmosphere with low pollution | - | Zinc | A | 10 |
| | - | Zn95%/Al5% alloy | A | 25 |
| | - | Zn90%/Al10% alloy | A | >50 |
| | Polyvinyl chloride (PVC) | Zn95%/Al5% alloy | A | >120 |
| | Polyamide (PA6) | | E | |
| | Polyvinyl chloride (PVC) | Zn90%/Al10% alloy | A | >120 |
| | Polyamide (PA6) | | E | |

| | | | | |
|---|---|---|---|---|
| **High aggressive: (C4)**<br>**Wet conditions**<br>Temperate zone, atmospheric environment with high pollution or substantial effect of chlorides, e.g. polluted urban areas, industrial areas, coastal areas, without spray of salt water, exposure to strong effect of de-icing salts e.g. subtropical and tropical zone, atmosphere with medium pollution industrial areas, coastal areas, shelter positions at coastline | - | Zn95%/Al5% alloy | A | 10 |
| | - | Zn90%/Al10% alloy | A | 25 |
| | Polyvinyl chloride (PVC) | Zn95%/Al5% alloy | A | 120 |
| | Polyamide (PA6) | | E | |
| | Polyvinyl chloride (PVC) | Zn90%/Al10% alloy | A | >120 |
| | Polyamide (PA6) | | E | |
| **Very High aggressive: (C5)**<br>**Wet conditions**<br>Temperate and subtropical zone, atmospheric environment with very high pollution and/or important effect of chlorides, e.g. industrial areas, coastal areas, shelter positions at coastline Subtropical and tropical zone (very high time of wetness), atmospheric environment with very high pollution SO2 (higher than 250 µg/m3) including accompanying and production ones and/or strong effect of chlorides, e.g. extreme industrial areas, coastal and off shore areas, occasionally contact with salt spray | Polyvinyl chloride (PVC) | Zn95%/Al5% alloy | A | 120 |
| | Polyamide (PA6) | | E | |
| | Polyvinyl chloride (PVC) | Zn90%/Al10% alloy | A | >120 |
| | Polyamide (PA6) | | E | |
| **Extreme aggressive: (CX)**<br>Subtropical and tropical zone (very high time of wetness), atmospheric environment with very high pollution SO2 (higher than 250 µg/m3) including accompanying and production ones and/or strong effect of chlorides, e.g. extreme industrial areas, coastal and off shore areas, occasionally contact with salt spray. | Polyvinyl chloride (PVC) | Zn90%/Al10% alloy | A | >120 |
| | Polyester (P)Polyamide (PA6) | | E | |

According to the aforementioned table, the five main categories are:

- Low Aggressive (C2)
- Medium Aggressive (C3)
- High Aggressive (C4)

- Very High Aggressive (C5)
- Extreme Aggressive (CX)

# 9 Calculation Example

A typical computation example according to the new approach examined in this scientific reference manual is presented as follows. This leads the user through Mac S-Design for a complete understanding of the calculation procedure and will be followed analytically.

As a general approach, the problem of the stability of the surficial soil layer of a slope can be addressed through three main phases of analysis:

- **Phase 1:**
  **Identification of the potential failure mechanism:**

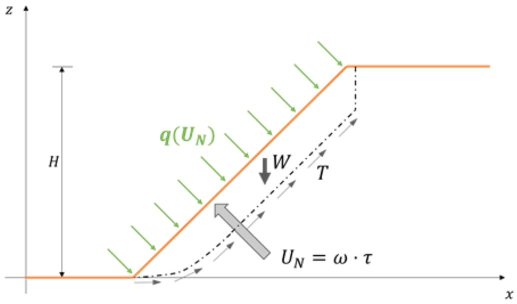


- Identification of both the “failure surface” and the related field of soil displacements **U(x, z)**;
- Analysis of driving forces and resisting forces;
- Instability due to slope angle, unstable soil layer and soil strength parameters, tension crack, water table depth, etc.

- **Phase 2:**
  **Stability Analysis:**

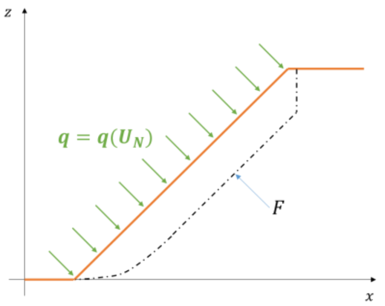


- Definition of the ‘q’ pressure needed to stabilize the slope.

- **Phase 3:**
  **Definition of the Characteristic curve:**

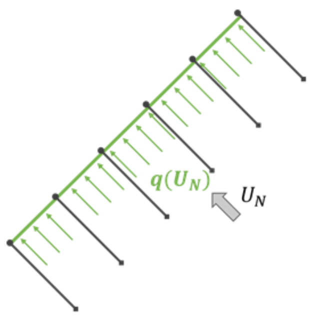


- The Characteristic curve can be defined;
- The pressure ‘q’ that shall be provided by the mesh is related to the Soil displacements U(x,z) and also depends on the applied product;
- The force acting on the anchor can be computed to ensure the equilibrium of the system.

These phases briefly explain how Mac S-Design addresses the stability of the surficial soil layer of a slope under study. It is vital to note that Mac S-Design does not consider the global stability of the soil slope and this must be analysed with different tools specifically designed for that purpose.

In the following paragraphs, a detailed explanation of the procedure will be provided highlighting the important method characteristics. The conceptual framework of Mac S-Design can be summarized in the following logical flow process (Figure 22). The procedure in the case of Approach 1 only is then summarized, as approach 2 is substantially similar.

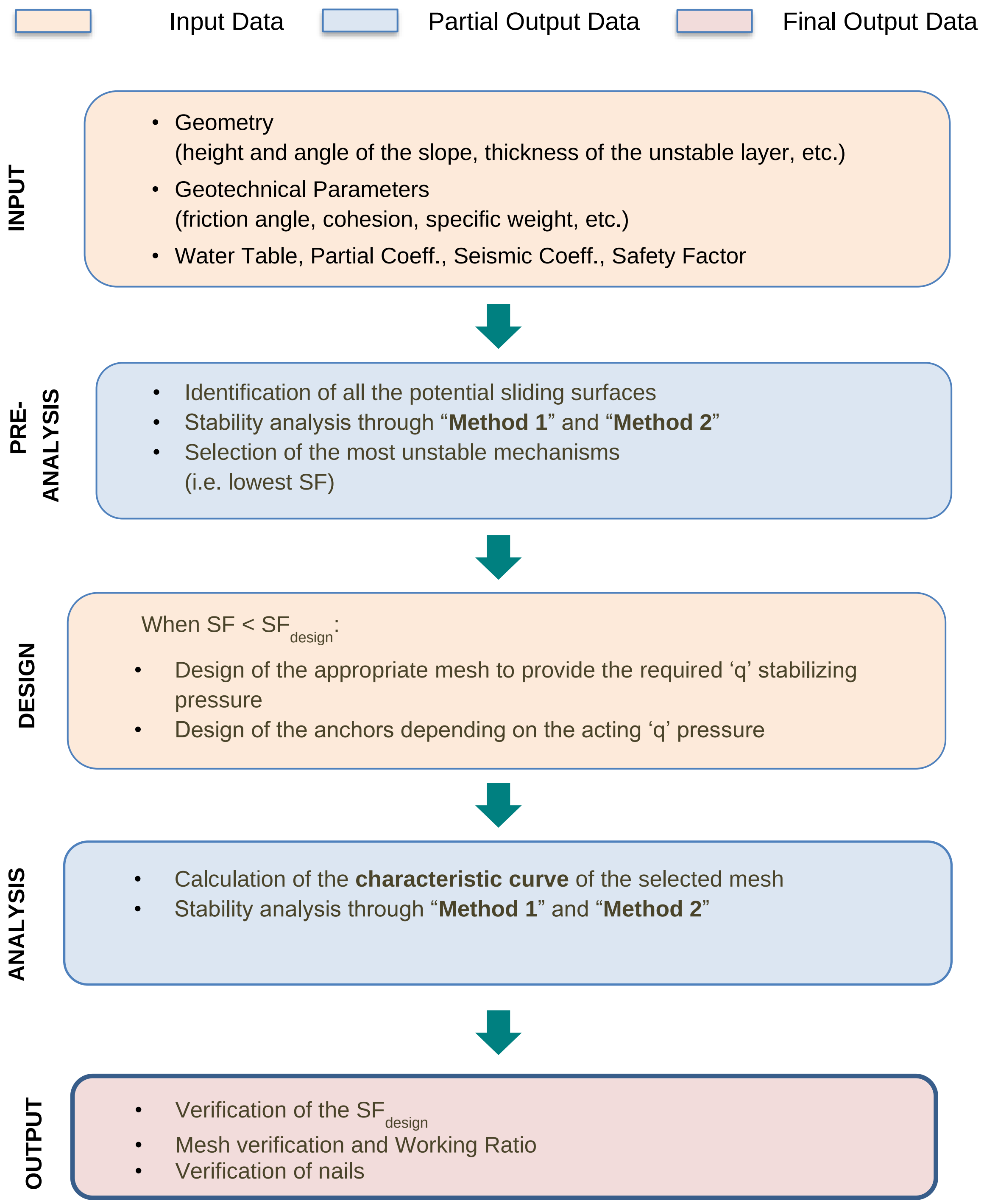


*Figure 22. Flow-process followed in Mac S-Design.*

Mac S-Design analyses all the potential mechanisms along the slope. Each mechanism is characterized by a P' point for which a corresponding surfacing point R can be identified. All the sliding surfaces (P''-R segment) of the base wedge are analysed thereafter, i.e. all the angles α are considered: the P'' point moves from P' down to the "toe point" accounting for all the potential critical surfaces that can occur.

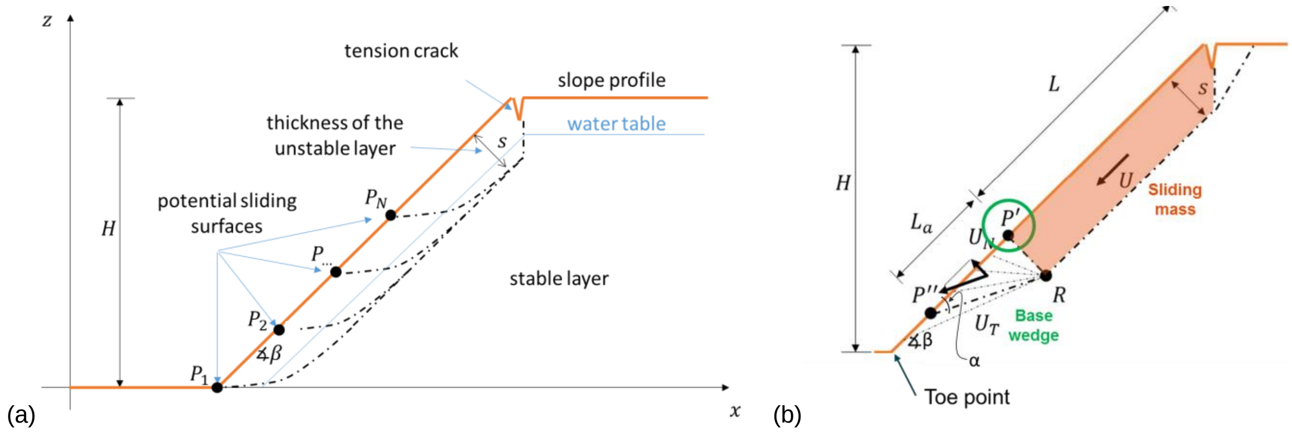


*Figure 23. (a) Scheme of all the P' point analysed along the slope and (b) detail of a specific mechanism and all the considered α angles.*

All the mechanisms along the slope are then analysed (Figure 23a) in order to identify the most unfavourable one. The calculation procedure for each mechanism (Figure 23b) can be subdivided in 4 main steps:

1. equilibrium of the upper sliding mass,
2. equilibrium of the base wedge,
3. generation and application of the characteristic curve,
4. final verification and output results.

- **Step 1: Equilibrium of the sliding mass:**

The equilibrium of the upper sliding mass can be imposed:

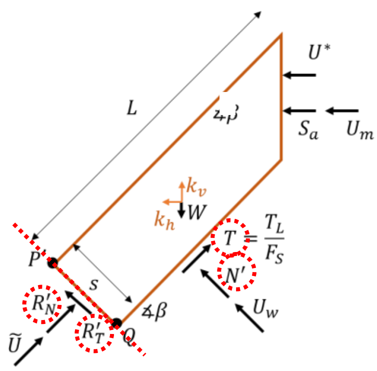


*Figure 24. Equilibrium scheme for the upper sliding mass.*

The input and output parameters used for the equilibrium are listed in the following

- ✓ *Input parameters:*

  W: as a unit weight's function

  $k_h$, $k_v$: seismicity input data

  $S_a$: active pressure as a geometrical parameter's function

  U*: pore pressure in tension crack

  $U_m$: water table pressure uphill sliding mass

  Ũ: water table pressure downhill sliding mass

- ✓ *Output parameters (highlighted in red in Figure 24):*

  $R'_N$, $R_T$: interface forces, as a FS function

  N', $T_L$: principal forces acting to the sliding mass

- **Step 2: Equilibrium of the base wedge:**

The computed equilibrium of the sliding mass then allows the equilibrium of the base wedge to be solved (Figure 25). For each P' point, all the α angles are considered, then all the base wedge elements varying the P'' points are analysed. P'' moves along the external surface from P' down to the toe of the slope. For each base wedge P'P''R the required stabilizing pressure q(α) is then computed.

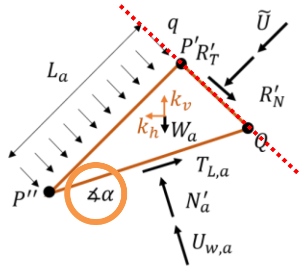


*Figure 25. Equilibrium scheme for the lower base wedge.*

- ✓ *Input Parameters (also computed in step 1):*

  $R'_N$, $R_T$: interface forces (as a FS function)

  N', $T_L$: principal forces acting to the sliding mass

- ✓ *Output parameters:*

  α: base wedge inclination (assumed as known variable through the iteration process)

  q(α): pressure required to stabilize the base wedge, i.e. identifying the weakest sliding plane for the base wedge

N'a, TL,a: principal forces acting on the base wedge

- **Step 3: Mesh verification:**

Having computed all the necessary equilibrium conditions for the slope being analysed, the mesh verification is next. The use of the characteristic curves enables this verification to be carried out as follows:

1. The pressure '**q**' required to stabilize the base wedge is determined in Step 2;
2. The tensile force "**F**" acting on the anchor can be computed from the equilibrium condition: $\boldsymbol{F}=\boldsymbol{q}\cdot(Area\ of\ Anchor\ Influence)$;
3. The actual force $\mathbf{F_{actual}}$ is verified to be within the limit of the **Characteristic curve** which is dependent upon the strength of the product ($\mathbf{T_{max}}$) defined on tensile force acting in the mesh;
4. The actual tensile force '$\mathbf{T_{actual}}$' acting on the mesh can be derived and compared with the strength of the product '$\mathbf{T_{max}}$'.

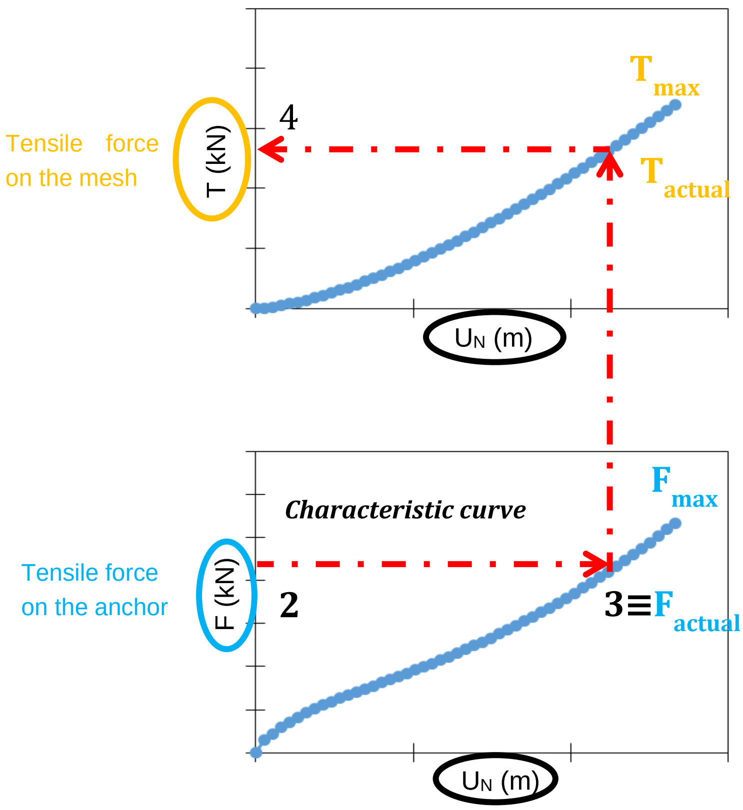


*Figure 26. Conceptual use of the characteristic curve for the mesh verification.*

- **Step 4: Output results:**

Once the equilibrium analysis is solved through the steps 1 to 3, the following outputs can be achieved:

- ✓ Verification of the target $FS_{design}$,
- ✓ Verification of the mesh expressed as a Working Ratio (%); the ratio between the actual pressure 'q' and the limit value of the related characteristic curve '$q_{max}$',
- ✓ Maximum loads applied on the Anchors (N, T, M) and their verifications:
  - M-N domain,
  - Design of the embedded length.

The variation of the input parameters then influences the output verifications. By keeping constant all the relevant parameters of the slope (i.e. geometry, mechanical parameters, etc.) the main parameters of the product or the nail pattern can be evaluated.

The use of a higher performance product enables a greater anchor spacing to be considered. This results in a higher Working Ratio of the mesh as well as in a higher force acting on the nails and an optimised solution will balance the technical, commercial and construction variables

# 10 References


Butterfield R. 1980. A simple analysis of the load capacity of rigid footings on granular materials. Journée de Géotechnique, ENTPE, Lyon, France, 128–137.

Cazzuffi D, Cardile G, Gioffrè D (2014). Geosynthetic engineering and vegetation growth in soil reinforcement applications. Transp Infrastruct Geotechnol 1:262–300.

Di Laora, R., Maiorano, R.M.S., Aversa, S. (2017). Ultimate lateral load of slope-stabilising piles. Géotechnique Letters 7, 237–244.

Fredlund, D.G., Rahardjo, H. (1993). Soil Mechanics for Unsaturated Soils. ISBN:9780471850083 |Online ISBN:9780470172759 |DOI:10.1002/9780470172759. Copyright © 1993 John Wiley & Sons, Inc.

Galli, A., Maiorano, R.M.S., di Prisco, C., Aversa, S. (2017). Design of slope-stabilizing piles: From Ultimate Limit State approaches to displacement-based methods. Rivista Italiana di Geotecnica, 51(3), pp. 77-93.

Hoffman, P. (2016). Contributions of Janbu and Lade as applied to Reinforced Soil. Proceedings of the 17th Nordic Geotechnical Meeting, 25th - 28th of May, Reykjavik.

Janbu, N. (1963). Soil Compressibility as Determined by Oedometer and Triaxial Tests, European Conference on Soil Mechanics and Foundation Engineering, Wiesbaden, Germany, Vol. 1, pp. 19-25.

Lade, P.V., and Nelson, R.B. (1987). Modelling the Elastic Behavior of Granular Materials, International Journal for Numerical and Analytical Methods in Geomechanics, 11, 521-542

Lancellotta R. (2012). Geotecnica. Ed. Zanichelli.

MACCAFERRI



**Officine Maccaferri S.p.A.**
Via J.F. Kennedy, 10
40069 Zola Predosa (Bologna) - Italy
**T:** + (39) 051 643 6000
**E:** info@hq.maccaferri.com

**maccaferri.com**